EVALUATION OF JET-ROOF GEOMETRY FOR SNOW-CORNICE CONTROL

By K. L. Dawson *and* T. E. Lang

(Department of Civil Engineering and Engineering Mechanics, Montana State University, Bozeman, Montana 59717, U.S.A.)

Abstract. Numerical hydrodynamic simulation of the jet-roof geometry for control of snow deposition to prevent cornice formation at mountain ridges is reported. Different jet-roof geometries are evaluated based upon the extent and size of the ground-surface stagnation region and the recirculation region to the lee of the roof. Results show that jet-roof length should be of the same order as nominal height of the roof from the ground surface. Efficient placement of the roof is shown to be that with the leading edge directly above the mountain ridge, and roof angle approximately equal to lee slope angle. In numerical simulation of flow-field start-up, near steady-state flow is approached in less than 1.0 s real time, indicating short transient-flow duration.

Résumé. *Estimation de la géométrie des toits-buse pour le contrôle des corniches de neige.* On rapporte un essai de simulation hydrodynamique numérique de la géométrie des toits-buse pour le contrôle du dépôt de la neige et pour empêcher la formation de corniches le long des crêtes montagneuses. On a comparé différentes géométries de toits-buse à partir de l'extension et de la forme de région de sol dénudé et de la région de recirculation sous le vent du toit. Les résultats montrent que la longueur du toit-buse devrait être de même ordre de grandeur que la hauteur nominale du toit au dessus de sol. On montre que l'emplacement efficace du toit doit être celui avec le bord d'attaque du toit directement au droit de la crête et l'angle du toit approximativement égal à l'angle de la pente du sol sous le vent du toit. Dans la simulation numérique du démarrage de la ventilation, un état voisin de l'état d'équilibre est atteint en moins d'une seconde de temps réel, prouvant que la durée de l'écoulement transitoire est courte.

Zusammenfassung. *Verwendung von Jetdachformen zur Steuerung von Schneewächten.* Es wird über eine numerische hydrodynamische Simulation der Jetdach-Geometrie zur Steuerung der Schneeablage mit dem Ziel, Wächtenbildung an Bergrücken zu verhindern, berichtet. Die Untersuchung erstreckt sich auf verschiedene Jetdachformen ausgehend von der Ausdehnung und Grösse des Stagnationsgebietes an der Grundfläche und der Rückzirkulation auf der Lee-Seite des Daches. Die Ergebnisse zeigen, dass die Länge der Jetdächer dieselbe Grössenordnung besitzen sollte wie die Nennhöhe des Daches über der Grundfläche. Als wirkungsvolle Aufstellung des Daches ergibt sich eine solche, bei der die Führungskante direkt über dem Bergrücken liegt; dabei sollte der Dachwinkel annähernd gleich der Hangneigung auf der Lee-Seite sein. Bei der numerischen Simulation des Ingangkommens eines Strömungsfeldes wird eine beinahe stetige Strömung in weniger als 1 s Echtzeit erreicht, was auf eine kurze Dauer der Übergangsströmung hinweist.

INTRODUCTION

From experimental and operational studies by Montagne and others (1968), Latham and Montagne (1970), Montagne (unpublished), and Burns (1974), the applicability of the "jet roof" to prevent snow-cornice formation to the lee of mountain ridge crests is well established. Under the conditions of prevailing wind, strategic placement of the roof near the ridge crest, and selection of the optimum roof geometry, the jet roof can be effective in directing air flow. The directed air flow is intended to scour the ground surface on the lee side of the ridge in order to transfer and spread the snow mass down-slope, instead of having it accumulate to the lee of the ridge in the form of a cornice. This distribution process makes avalanche control easier, and avalanches triggered by cornice fall are prevented. The jet roof can be idealized as a flat surface supported 3.0 to 4.0 m above the ground surface at the leading edge, and located at or slightly windward of the ridge crest.

Starting with a geometric configuration of the jet roof as described above, a numerical hydrodynamic model of the flow problem was developed. Basic parameters varied in studying flow past the jet roof included the (1) slope-parallel length of the jet roof, (2) angular inclination of the jet roof relative to the lee slope, and (3) position of the roof relative to the ridge crest of the mountain. The two-dimensional evaluation of air flow past the roof is carried out using a modified version of the digital computer code SOLA, recently reported by Hirt and others (1975), in which laminar, viscous, incompressible, transient flow can be modeled.

The flow evaluation is confined to interpretation of velocity-vector plots of the flow field, for which local regions of stagnation and recirculation are compared for different roof geometries. A criterion is established to evaluate different geometries, and to assess the time required to reach quasi-steady-state flow. In using a laminar flow model, it is assumed that steadiness of the flow is a more dominant characteristic in establishing scour and stagnation regions than possible flow turbulence.

GOVERNING EQUATIONS AND PROBLEM SIMULATION

The governing equations that are to be solved numerically are the two-dimensional Navier–Stokes equations given by

$$\left.\begin{array}{l} \dfrac{\partial u}{\partial t}+\dfrac{\partial u^2}{\partial x}+\dfrac{\partial uv}{\partial y} = -\dfrac{\partial p}{\partial x}+g_x+\nu\nabla^2 u, \\[2ex] \dfrac{\partial v}{\partial t}+\dfrac{\partial uv}{\partial x}+\dfrac{\partial v^2}{\partial y} = -\dfrac{\partial p}{\partial y}+g_y+\nu\nabla^2 v, \end{array}\right\} \tag{1}$$

where u and v are velocity components in the x and y directions respectively, g_x and g_y are components of gravity, p is the ratio of pressure referred to constant fluid density, ν is the kinematic viscosity, and $\nabla^2 = \partial^2/\partial x^2+\partial^2/\partial y^2$ is the Laplacian operator. A finite difference form of Equations (1) combined with the physical conditions of zero divergence of fluid imposed at each cell by the continuity of mass equation, namely

$$\mathbf{\nabla}\cdot\mathbf{V} = \dfrac{\partial u}{\partial x}+\dfrac{\partial v}{\partial y} = 0, \tag{2}$$

comprise the solution algorithm developed by Hirt and others (1975). Modifications made to the SOLA code to adapt it more efficiently to the jet-roof problem are outlined in detail by Dawson and Lang (1979). A listing of the code designated JETROOF, is on file at the Rocky Mountain Forest and Range Experiment Station, 240 West Prospect Street, Fort Collins, Colorado 80521, U.S.A.

Three refinements were involved in the final representation of the jet-roof geometry (Fig. 1). Initially, a full-ridge model was used to evaluate the characteristic flow pattern. By inputting identical left boundary velocity components from the full-ridge model, the half-ridge and no-ridge models duplicated the flow patterns to sufficient accuracy; yet with a significant reduction in the number of cells, and considerable simplification in representation of the boundary constraints. The lower boundary of the final no-ridge model is slip-free parallel to the boundary and rigid normal to the boundary. The remaining three boundaries are continuative flow boundaries as defined by Hirt and others (1975). The leading edge of the jet roof is located 3.75 m from the ground surface for all computer simulations. Square cells 0.5 m on a side were determined to be near-optimum in providing accurate representation of the flow. Finer grids gave basically the same velocity profiles, yet coarser grids resulted in significant loss of accuracy. A typically developed flow field, showing the type of pictorial

| (a) FULL-RIDGE MODEL. | (b) HALF-RIDGE MODEL | (c) NO-RIDGE MODEL |
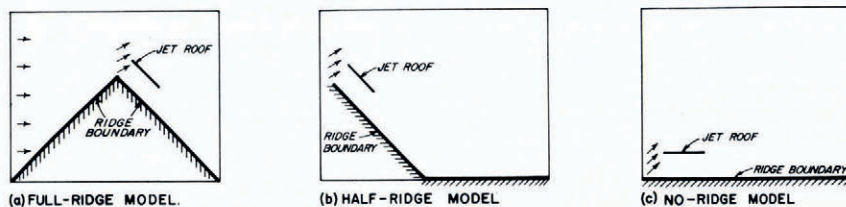
Fig. 1. Successive problem-simulation refinements of the jet-roof–mountain geometry.

output obtained from the computer simulations, is shown in Figure 2. Velocity vectors for each cell collectively depict the flow field past the solid-line jet roof. The dotted lines show the interpreted boundaries of the recirculating eddy at the trailing edge of the roof and the stagnation region at the ground surface. Initial simulations of the no-ridge model, made with a reduced number of cells above the roof as an economy measure, resulted in numerical instability due to the condition of large-magnitude, opposite-signed velocities occurring in adjacent cells at the upper continuative flow boundary. This first manifested itself in excessive iterations required to satisfy the incompressibility condition (Equation (2)), followed by complete divergence in local numerical accuracy. This instability is eliminated with the model of Figure 2, with eight cells vertically above the jet roof. Similar flow plots for all jet-roof geometries evaluated in this study are listed by Dawson and Lang (unpublished).
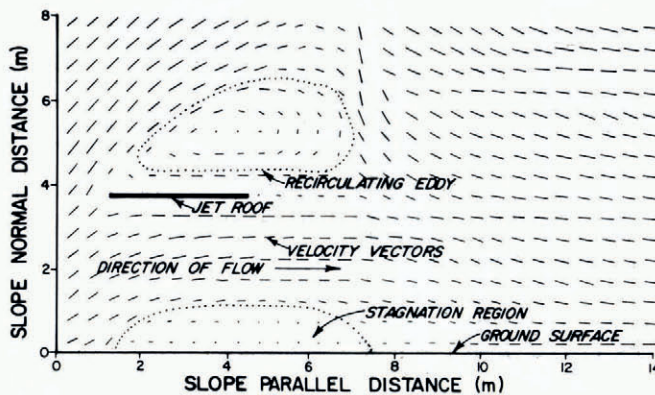
Fig. 2. *Flow field for the no-ridge model with a slope-parallel jet roof, 3.5 m characteristic length.*

RESULTS FROM COMPUTED DATA

Flow initiation in the JETROOF program is set by assigning to all flow cells of the no-ridge model the velocity components obtained from the column of cells at the leading edge of the jet roof of the full-ridge model. For the particular case considered, a 20 m/s input velocity at the left flow boundary is used. A mass-flow balance is achieved in each cell to a user-specified accuracy after each cycle. Only the left boundary of cells of the no-ridge model retain the original full-ridge velocities, which is the essential property of the continuative boundary condition. The flow is allowed to continue to CYCLE 100, which in all cases approaches steady-state flow.

As a means of quantifying the transient part of the developing flow, a non-dimensional velocity ratio is computed as part of the program output. This ratio, designated Ψ, is the average of the velocity magnitudes of the column of cells beneath the leading edge of the jet roof divided by the average of the velocity magnitudes at the trailing edge for the corresponding cells. For different slope-parallel jet-roof lengths, the velocity ratio Ψ is plotted versus time in Figure 3. The jet-roof length has a decided effect upon initial flow perturbation and the plot shows the characteristic of damped transients tending toward steady-state, with all lengths requiring 0.8 to 1.0 s real time for transient subsidence.

Selecting a jet-roof length of 3.0 m as representative, later to be shown to be near-optimum, Ψ is plotted versus time for various angles of roof inclination relative to the ground surface (Fig. 4). From these results it is seen that the approach to steady-state flow is different for positive and negative angles of inclination. The positive-angle flows tend to stabilize in 0.8 to 1.0 s with the average leading-edge velocity greater than the corresponding trailing-edge
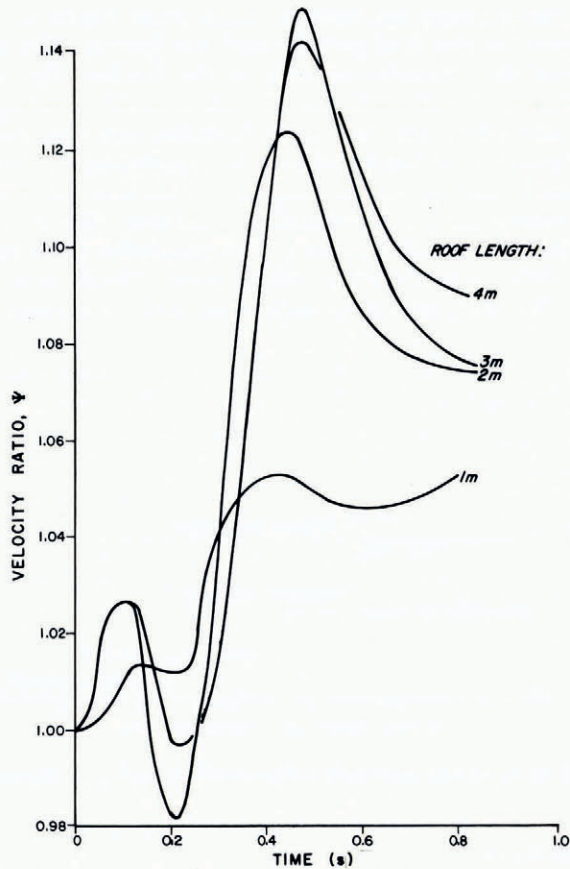
Fig. 3. Ratio of average leading-edge velocity to average trailing-edge velocity, Ψ, versus time into developing flow for different lengths of slope-parallel jet roofs.

value. The negative angle flows tend to stabilize in 0.5 to 0.6 s. In the case of negative angles, the average trailing edge velocity exceeds that of the leading edge, which enhances the effect of the air flow to scour the ground surface.

A second aspect of jet-roof evaluation is to compare the size and orientation of the stagnation region and recirculating eddy (Fig. 2) for different roof geometries. A large recirculating eddy causes excessive snow deposition down-stream of the jet roof. A large stagnation region results in ground-surface deposition and possible complete sealing of the area beneath the roof. A recirculation in close proximity of the roof can cause snow deposition and build-up on the roof which can cause structural collapse.

Plots of recirculation and stagnation regions for the slope-parallel roof of various lengths are shown in Figure 5, for a jet roof of 3.0 m in length at various negative inclinations in Figure 6, and for various positive inclinations in Figure 7. Based upon the criteria cited, the optimum design of the roof appears to be one at a small negative inclination and on the order of 3.0 m in length, for the input conditions examined. This result is based in part upon the information of Figure 4, which indicates that the velocity intensification in the scour region which occurs with negative inclinations is desirable. Large negative inclinations produce a large recirculating eddy, which can cause excessive down-stream deposition, particularly if the prevailing wind is not steady.
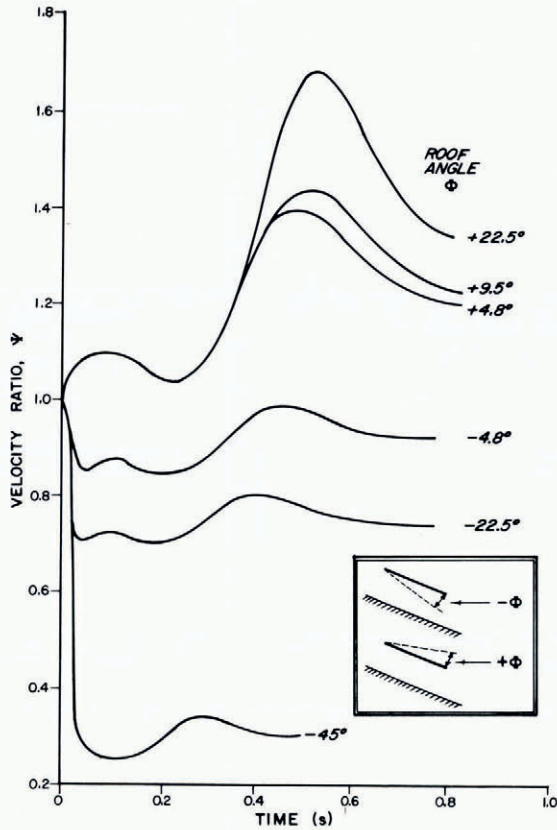
Fig. 4. Ratio of average leading-edge velocity to average trailing-edge velocity, Ψ, versus time into developing flow for different angles of inclination of a jet roof 3.0 m long.

Our final evaluation is in regard to the position of the jet roof relative to the mountain ridge. Using a jet-roof configuration of length 3.0 m and inclination angle to the lee slope of $\phi = 0°$, we consider four positions of the roof, as depicted in Figure 8a. The four configurations are selected such that the shortest normal distance from the leading edge of the roof to the ridge surface is 3.0 m. The recirculation regions and the leading edge of the stagnation regions for the four cases are shown in Figure 8b. The recirculation regions show a trend toward smaller regions from Case A to Case D; however, this variation is not considered significant in selecting one configuration over another. From the standpoint of wanting the stagnation region as far down the slope as possible, Cases B and C are preferred. To further appraise these cases, the average velocity at the trailing edge of the jet roof, and the volume flow-rate per unit width of jet roof are computed and summarized in Table I. It is determined from these results, that although the average velocity for Case B is 7% lower than that of Case C, the volume flow-rate for Case B is 33% greater than that of Case C. The greater flow-rate for Case B is principally a function of the greater area of the opening at the trailing edge of the jet roof, which provides a greater margin against possible snow blockage under the roof. In accounting for all aspects of the jet-roof configurations evaluated, Case B, for which the leading edge of the jet roof is directly above the ridge crest, has characteristics most desirable from a design standpoint. Since most jet-roof configurations tested to date have
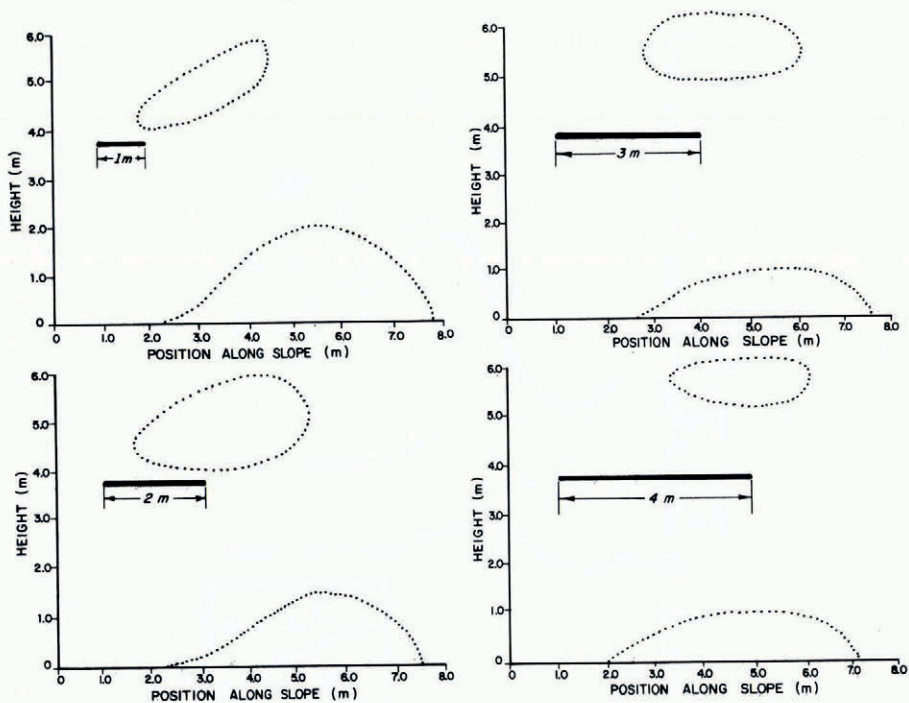
Fig. 5. *Dependence of stagnation region and recirculating eddy upon slope-parallel jet roof.*
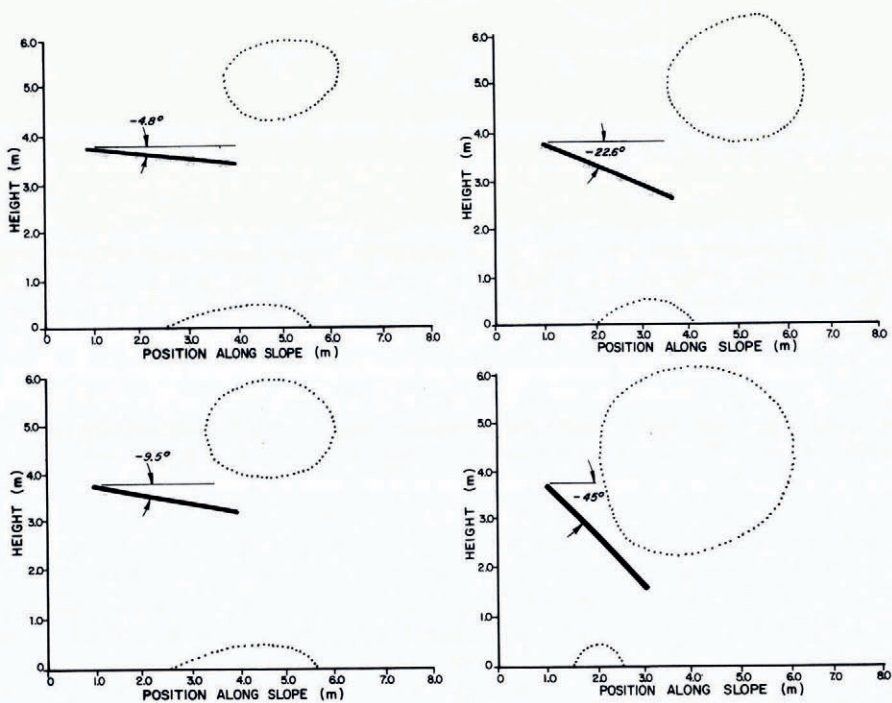
Fig. 6. *Dependence of stagnation region and recirculating eddy upon negative jet-roof inclination for a jet roof 3.0 m long.*

been oriented as in Case D (Perla and Martinelli, 1976, p. 156), further computer simulation and experimental verification of the Case B configuration is warranted. In such cases, particular attention should be given to the apparent relationship between the average trailing-edge velocity of the jet roof, and the volume flow-rate per unit width of jet roof.
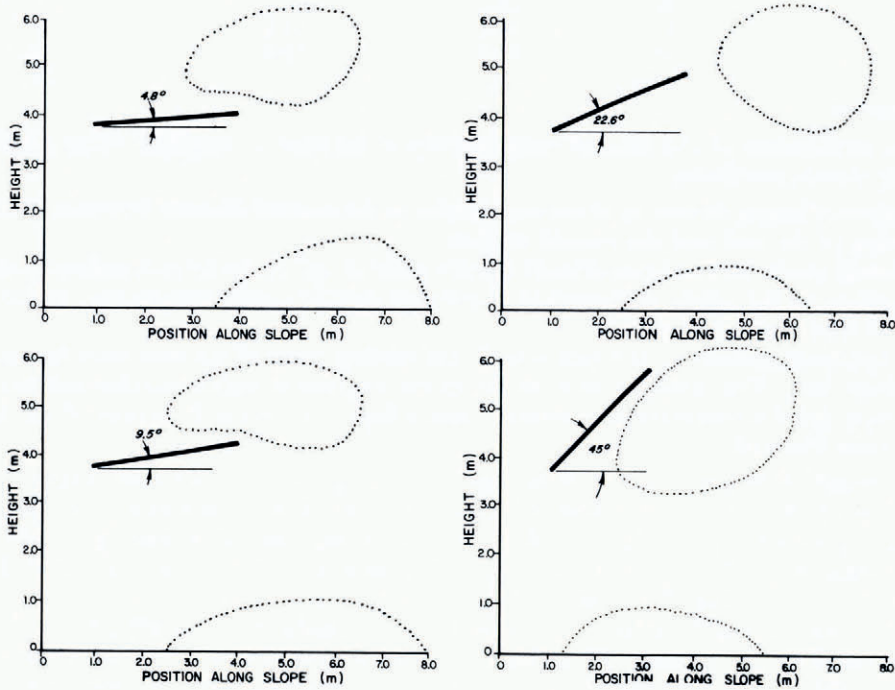
Fig. 7. *Dependence of stagnation region and recirculating eddy upon positive jet-roof inclination for a jet roof 3.0 m long*

(a)

(b)
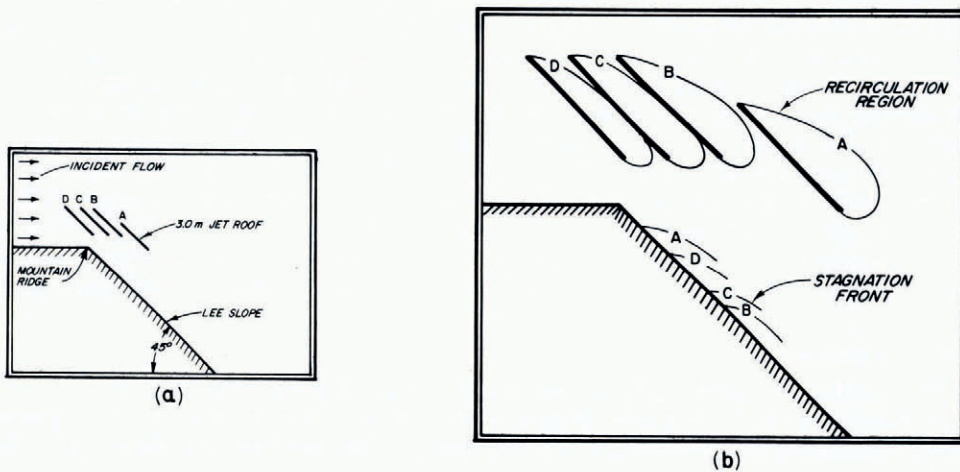
Fig. 8. (a) *Definition of four jet-roof geometries relative to the mountain ridge, and (b) stagnation regions and recirculating eddies for the four regions.*

TABLE I. AVERAGE VELOCITY AND VOLUME FLOW-
RATE AT THE VERTICAL CROSS-SECTION AT THE
TRAILING EDGE OF THE JET ROOF

Case	Average velocity $m\ s^{-1}$	Volume flow-rate $m^3\ s^{-1}$
A	13.9	48.8
B	18.6	43.3
C	19.9	30.4
D	20.2	15.9

CONCLUSIONS

Flow evaluations of the jet-roof configuration at or near a mountain ridge provide the following design conditions:

1. Jet-roof length should be of the same order as the normal distance between the leading edge of the roof and the ground surface.
2. Small clockwise rotations (Fig. 6) on the order of 10° of the jet roof enhances scouring action by the wind, evidenced in a reduced ground-surface stagnation region and a reduced recirculating eddy.
3. Optimum position of the roof is with the leading edge of the roof directly above the ridge line. This configuration results in the stagnation region starting farthest down-slope (of the configurations tested), and a high volumetric flow-rate of air diverted under the roof.

The length of the jet roof controls principally the height of the stagnation region, while the inclination of the roof controls both its length and position. Large clockwise inclinations continue to reduce the stagnation region, but at the sacrifice of increasing the size of the recirculating eddy. This in turn causes excessive snow deposition down-stream of the roof, but with little spreading effect (Montagne and others, 1968). Steady flow is approached in 0.8 to 1.0 s for the slope-parallel roof geometry, and is reduced 20 to 30% by inclining the roof at a small clockwise angle. Thus, long-duration computer simulations are unnecessary in evaluating different design configurations. The exception would be in evaluating a fluctuating flow condition, an option which can be incorporated in JETROOF, but with a corresponding increase in cost due to excessive iterations in order to evaluate continuing transients.

Reduction of the SOLA code to more specific, special forms like JETROOF is efficient and practical when the application warrants a large number of case evaluations. The SOLA code is organized and written in a format conducive for reduction, an apparent foresight recognized by the authors of the code. Besides code editing and modification, two other refinements contributed to efficiency in the jet-roof study. One is the fortunate dynamic similarity of flows between the full-, half-, and no-ridge models. This resulted in an order-of-magnitude reduction in computer simulation cost. The second is the determination that 7 to 10 cells between the ground surface and roof, and between the roof and the upper continuative boundary, are necessary and sufficient for representative modeling of the flow. With this cost weighed against the efforts that must go into a comparable experimental program, merit of applying the SOLA code to other aspects of snow mechanics is both warranted and encouraged.

REFERENCES

Burns, T. J. 1974. Jet roofs for snow cornice prevention at Carson Spur. *State of California. Dept. of Transportation. Research Report* No. CA-DOT-DIST. 10-601101-1-74-1.

Dawson, K. L., *and* Lang, T. E. 1979. Numerical simulation of jet-roof geometry for snow cornice control. *U.S. Dept. of Agriculture. Forest Service. Research Paper* RM206.

Dawson, K. L., *and* Lang, T. E. Unpublished. Listings of flow field plots from numerical simulation of air flow past jet roof geometries for snow cornice control. [Compiled for U.S. Forest Service. Rocky Mountain Forest and Range Experiment Station, Fort Collins, Colorado 80521, 1977.]

Hirt, C. W. 1968. Heuristic stability theory for finite-difference equations. *Journal of Computational Physics*, Vol. 2, No. 4, p. 339–55.

Hirt, C. W., *and others*. 1975. SOLA—a numerical solution algorithm for transient fluid flow, by C. W. Hirt, B. D. Nichols, and N. C. Romero. *Los Alamos Scientific Laboratory. Report* No. LA-5852.

Latham, J., *and* Montagne, J. 1970. The possible importance of electrical forces in the development of snow cornices. *Journal of Glaciology*, Vol. 9, No. 57, p. 375–84.

Montagne, J. Unpublished. Snow cornices and devices for their control. [Written for Atwater Avalanche Honorarium, Yosemite Park, California, 1973.]

Montagne, J., *and others*. 1968. The nature and control of snow cornices on the Bridger Range, southwestern Montana, by J. Montagne, J. T. McPartland, A. B. Super, and H. W. Townes. *U.S. Dept. of Agriculture. Forest Service. Alta Avalanche Study Center. Miscellaneous Report* 14. [Available from Rocky Mountain Forest and Range Experiment Station, Fort Collins, Colorado 80521.]

Perla, R. I., *and* Martinelli, M., *jr.* 1976. Avalanche handbook. *U.S. Dept. of Agriculture. Forest Service. Agriculture Handbook* 489.